Supplement of

Impact of temperature on the role of Criegee intermediates and peroxy radicals in dimers formation from β-pinene ozonolysis

Yiwei Gong[1,2], Feng Jiang[2], Yanxia Li,[2] Thomas Leisner[2,3], and Harald Saathoff[2]

[1]Department of Atmospheric and Oceanic Sciences, School of Physics, Peking University, Beijing, China
[2]Institute of Meteorology and Climate Research, Karlsruhe Institute of Technology, Karlsruhe, Germany
[3]Institute of Environmental Physics, Heidelberg University, Heidelberg, Germany

Correspondence to: Yiwei Gong (yiwei.gong@kit.edu) and Harald Saathoff (harald.saathoff@kit.edu)

Table S1. Main updates to the formation of β-pinene-derived Criegee intermediates suggested for MCM v3.3.2.

No.	Modified reaction	Branching ratio in MCM	Updated branching ratio	Reference
1	BPINENE + O3–>NOPINONE + CH2OOF	0.40	0.20	Ma and Marston, 2008; Nguyen et al., 2009; This work
2	BPINENE + O3–>NOPINOOA + HCHO	0.60	0.80	Ma and Marston, 2008; Nguyen et al., 2009; This work
3	CH2OOF–>CH2OO	0.37	0.50	Ahrens et al., 2014; Winterhalter et al., 2000; Zhang and Zhang, 2005
4	CH2OOF–>HO2+CO+OH	0.13	0.30	Atkinson et al., 1992; Nguyen et al., 2009
5	CH2OOF–>CO	0.50	0.20	This work
6	NOPINOOA–>NOPINOO	0.17	0.40	Ahrens et al., 2014; Winterhalter et al., 2000; Zhang and Zhang, 2005
7	NOPINOOA–>NOPINDO2 + OH	0.50	0.30	Atkinson et al., 1992; Nguyen et al., 2009
8	NOPINOOA–>C8BC	0.33	0.30	This work

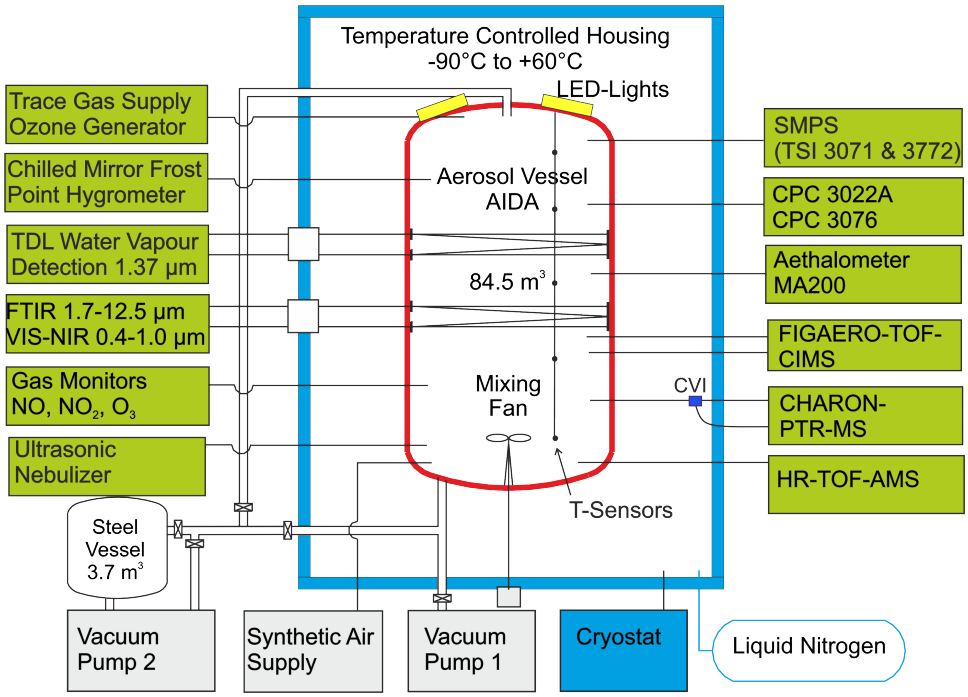

Figure S1. Schematic of the AIDA simulation chamber with the typical instrumentation.

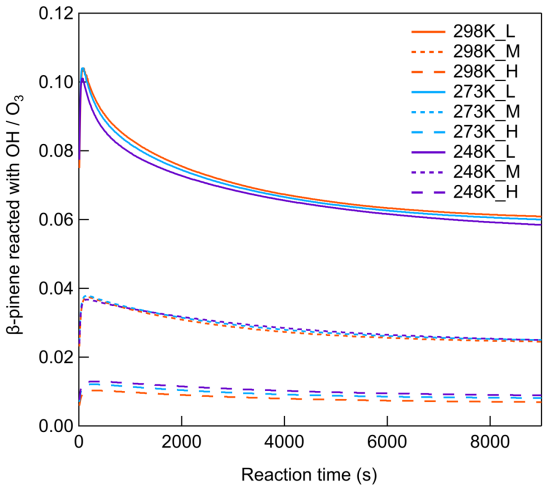

Figure S2. The ratio of the accumulated amount of β-pinene reacted with OH versus O_3 at different $[HO_2]/[RO_2]$ conditions and different temperatures (Exp. 298abc, 273abc, 248abc).

25

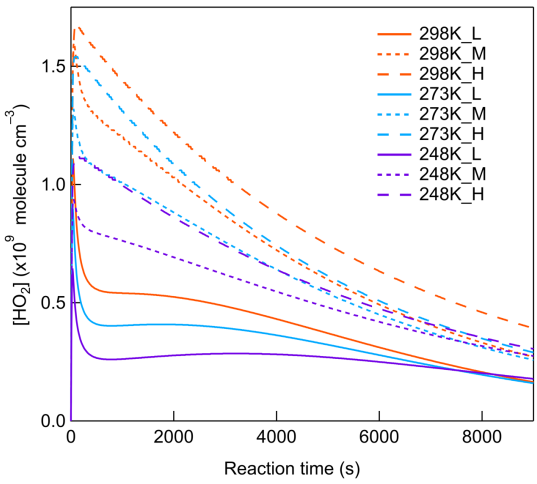

Figure S3. Simulated HO_2 concentration as a function of reaction time at different $[HO_2]/[RO_2]$ conditions and different temperatures (Exp. 298abc, 273abc, 248abc).

30

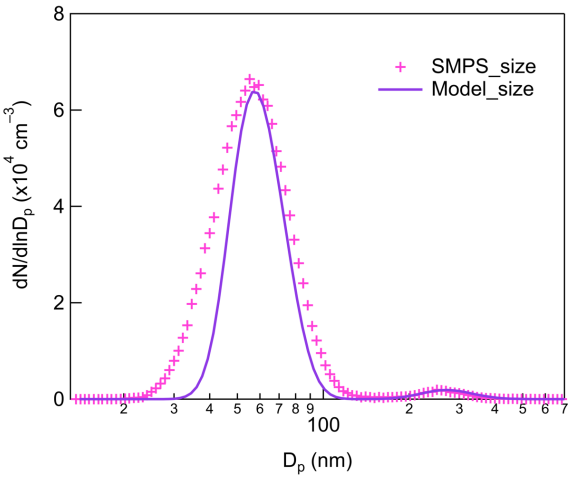

Figure S4. Particle size distribution from SMPS measurement and COSIMA model result at 7000 s of reaction (Exp. 298a).

35

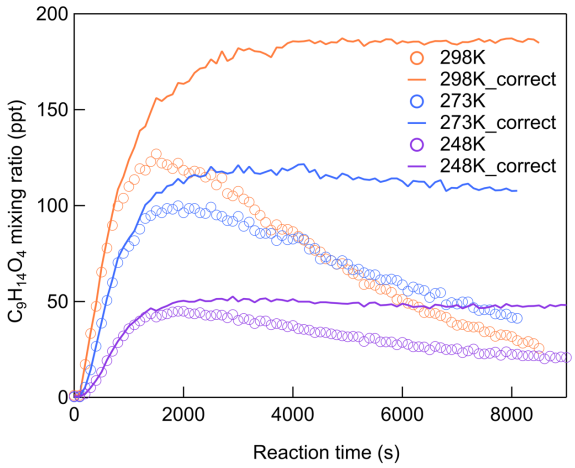

Figure S5. The mixing ratio of gas-phase $C_9H_{14}O_4$ before (measured) and after wall loss correction (modeled) at different temperatures (Exp. 298a, 273a, 248a).

40

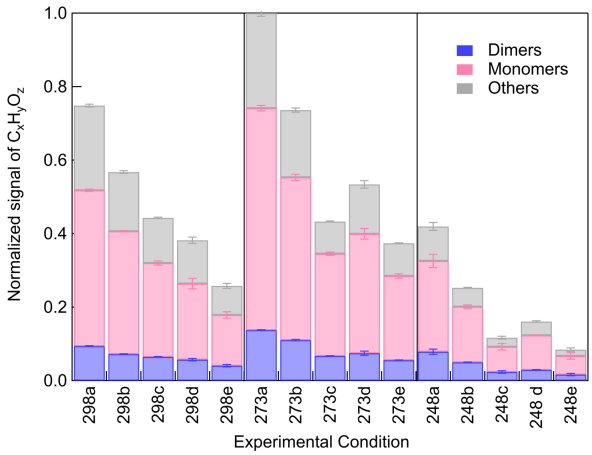

Figure S6. Normalized signals of all particle-phase $C_xH_yO_z$ compounds for different experimental conditions.

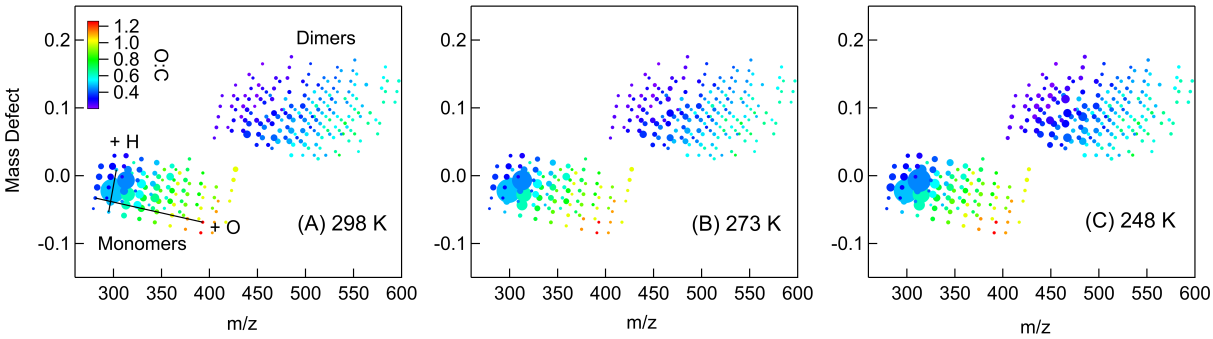

45

Figure S7. Mass defect plots of particle-phase monomers and dimers (with I^-) at different temperatures (Exp. 298a, 273a, 248a). Markers are sized by the square root of their signals and colored by the O/C ratio.

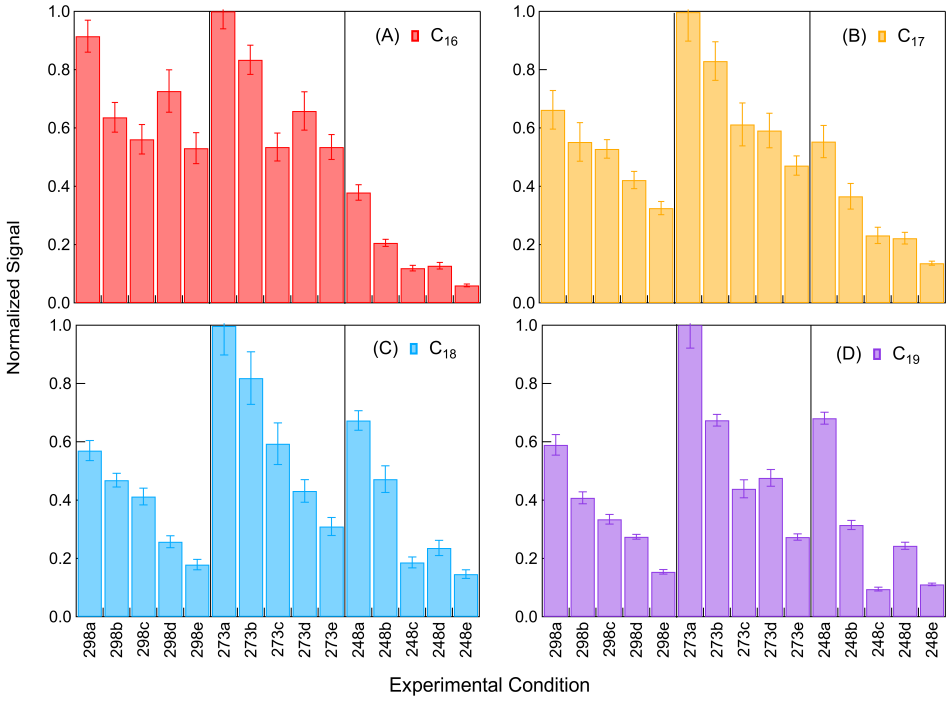

Figure S8. The particle-phase signals of (A) C_{16} (B) C_{17} (C) C_{18} (D) C_{19} dimers normalized to the peak intensity under different experimental conditions.

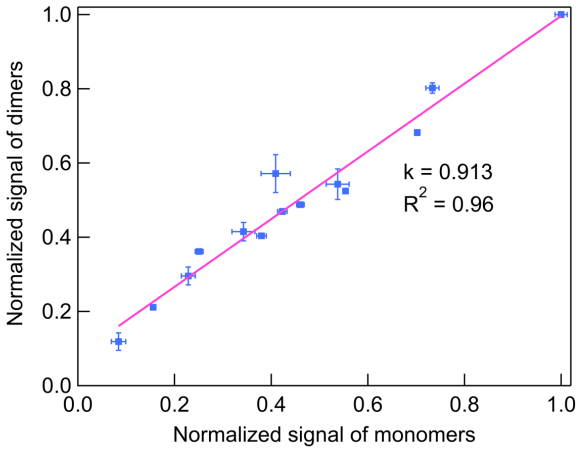

Figure S9. The correlation between particle-phase normalized signal of dimers with normalized signal of monomers. The solid line shows a linear fit.

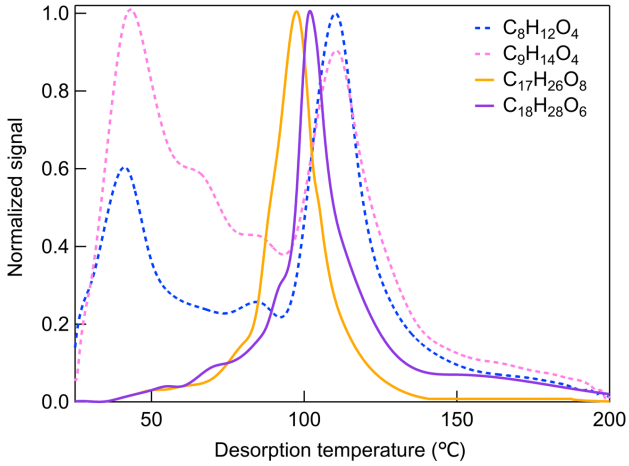

Figure S10. Thermograms of abundant monomers ($C_8H_{12}O_4$ and $C_9H_{14}O_4$) and dimers ($C_{17}H_{26}O_8$ and $C_{18}H_{28}O_6$), i.e., the normalized signals versus desorption temperature.

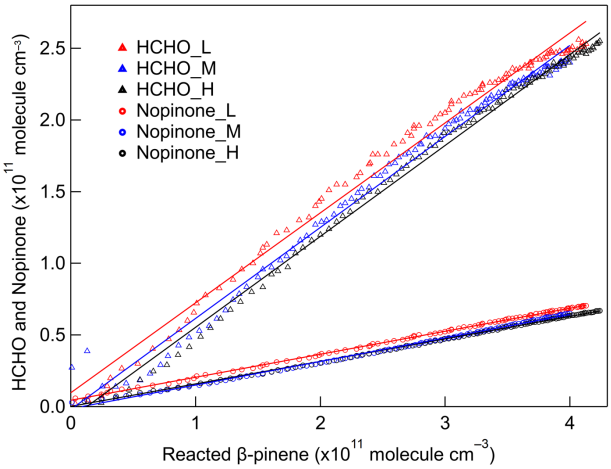

Figure S11. The formation of formaldehyde (HCHO) and nopinone as a function of β-pinene reacted at 298 K for different $[HO_2]/[RO_2]$ (Exp. 298abc). The lines represent linear fits and R^2 values are larger than 0.95.

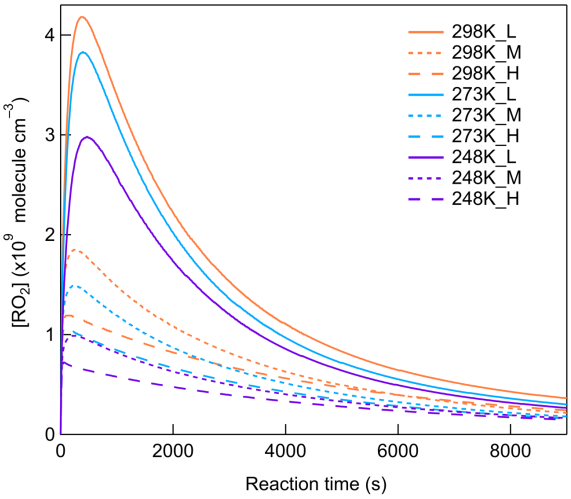

Figure S12. Simulated RO_2 concentration as a function of reaction time at different $[HO_2]/[RO_2]$ conditions and different temperatures (Exp. 298abc, 273abc, 248abc).

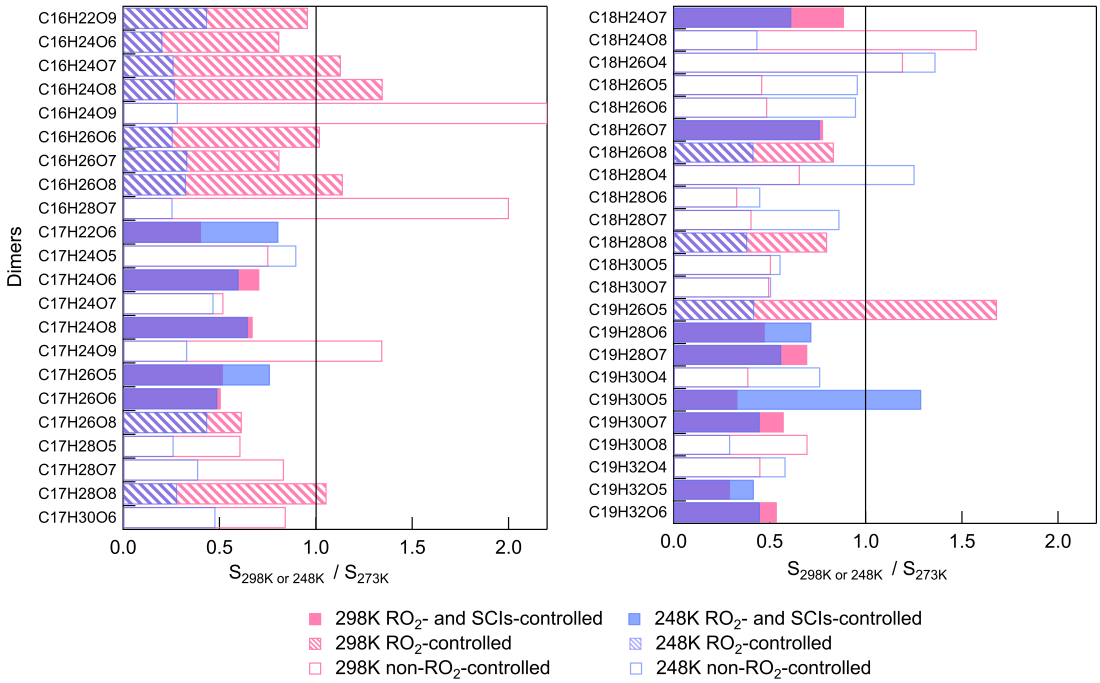

Figure S13. The relative changes of RO_2-controlled and non-RO_2-controlled abundant dimers at 298 K or 248 K versus 273 K (The relative standard deviations are within 25 %).

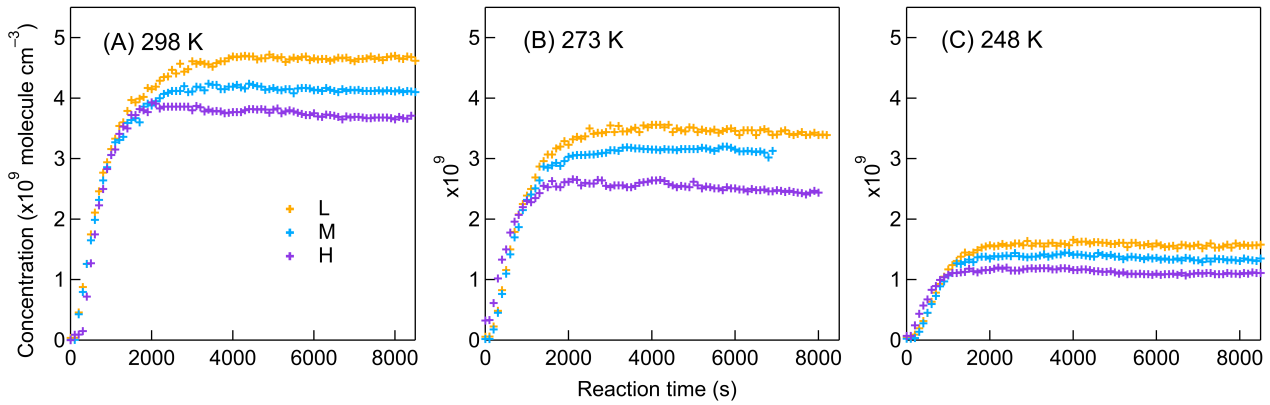

Figure S14. The impact of $[HO_2]/[RO_2]$ on the gas-phase concentrations of $C_9H_{14}O_4$ at (A) 298 K (B) 273 K (C) 248 K after wall loss correction (Exp. 298abc, 273abc, 248abc).

90